research articles Journal of proteome research

Analysis of Root Plasma Membrane Aquaporins from *Brassica oleracea*: Post-Translational Modifications, *de novo* Sequencing and Detection of Isoforms by High Resolution Mass Spectrometry

J. Casado-Vela,[†,‡,§] B. Muries,[†,||] M. Carvajal,[||] I. Iloro,[‡] F. Elortza,[‡] and M.C. Martínez-Ballesta*[,||]

Plataforma de Proteómica, CIC bioGUNE, CIBERehd, ProteoRed, Parque Tecnológico de Bizkaia, Edifício 800, 48160, Bizkaia, Spain, and Departamento de Nutrición Vegetal, Centro de Edafología y Biología Aplicada del Segura - CSIC, Apdo. Correos 164, 30100 Espinardo, Murcia, Spain

Received December 14, 2009

Plasma membrane Intrinsic Proteins (PIPs), a subfamily of aquaporins, are ubiquitous membrane channel proteins that play a crucial role in water uptake in plants. The use of high-performance liquid chromatography coupled to tandem mass spectrometry (HPLC−MS/MS) analysis of peptides has previously shown to be a valuable tool to differentiate among PIP homologues sharing a high sequence homology and also to characterize their post-translational modifications (PTMs). The recent introduction of mass spectrometers able to measure peptide mass with high mass accuracy, together with new alternative ways of peptide fragmentation allows the identification and characterization of proteins from nonsequenced organisms, such as broccoli. In this study, we combined three endoproteases (trypsin, Glu-C and Lys-C) with HPLC−MS/MS analysis and two types of peptide fragmentations, CID (collision induced dissociation) and HCD (higher-energy C-trap dissociation), to identify PIP isoforms and PTMs from broccoli roots. After *de novo* sequencing analysis, eight peptides showing homology to *Arabidopsis thaliana* PIPs were identified. Although *Arabidopsis* nomenclature of PIP isoforms has not been defined for broccoli, our results agree with the occurrence of seven AtPIP isoforms (PIP 1;1, PIP 1;2, PIP 1;3 and PIP2;2, PIP 2;3, PIP2;1 and PIP2;7) in broccoli roots, as compared to the plant model *A. thaliana.* To our knowledge, these results represent the deepest characterization of the PIPs isolated from the roots of broccoli, a crop with increasing agronomical interest.

Keywords: *Brassica oleracea* • plasma membrane intrinsic protein • *de novo* sequencing • LTQ Orbitrap • post-translational modifications

Introduction

Plant roots show a remarkable capacity to adapt to the physiological water demand of the whole plant and can quickly alter their water permeability as a response to several environmental stresses.[1] This ability to regulate water flow through cellular membranes is controlled by membrane protein channels, generally termed aquaporins, which belong to the major intrinsic protein (MIP) family.[2] Plant aquaporins can be classified into four subfamilies, plasma membrane intrinsic proteins (PIPs), tonoplast intrinsic proteins (TIPs), NOD26-like intrinsic proteins (NIPs) and small basic intrinsic proteins (SIPs).[3,4] PIPs share a similar structure, having the N- and C-terminal tails in the intracellular space, six transmembrane domains, three extracellular loops (termed A, C and E) and two intracellular loops (B and D).[5,6] In most of the plant species investigated, pharmacological and/or genetic experiments evidence that PIPs represent the most important pathway for water uptake by roots.[7]

Genome sequencing experiments led to the identification of 13 genes encoding for PIPs in the model plant *Arabidopsis thaliana*, from the Brassicaceae family.[1,4] Eleven from those 13 expressed genes have been identified in *Arabidopsis* using PCR experiments.[8] A similar number of genes encode for PIPs in rice and maize (11 and 13 genes, respectively),[2,9] two plant species widely commercialized. The finding of different gene products encoding for PIPs suggests that PIPs may play different roles in plants. Therefore, further research leading to the identification and characterization of PIPs in different plant species and the screening of their expression in different organs may help to unravel the regulation of PIPs in plants.[6] Nevertheless, the identification of the expression of PIPs is not sufficient because the activity and permeability of PIPs is regulated by post-translational modifications (PTMs).[10] Thus, several recent works have significantly enhanced the description of plant aquaporin phosphorylation, suggesting that it could favor an open-pore state.[11,12] However, the results are sometimes contradictory and a critical issue is to identify among the many

* Corresponding author: María del Carmen Martínez-Ballesta, Departamento de Nutrición Vegetal., Centro de Edafología y Biología Aplicada del Segura - CSIC., Apdo. Correos 164, 30100 Espinardo, Murcia, Spain. Tel: +34 968 39 62 29. Fax: +34 968 39 63 13. E-mail: mballesta@cebas.csic.es.

† These authors contributed equally to the paper.

‡ CIBERehd.

§ Current address: TCD Pharma, Centro Nacional de Biotecnología, Translational Oncology Unit, lab. 35. C/Darwin 3, Madrid, Spain.

|| CSIC.

10.1021/pr901150g

Published on Web 05/12/2010

predicted phosphorylation sites those that are biochemically and functionally relevant. Also, the functional role of the phosphorylation sites, in aquaporin gating or trafficking, needs to be elucidated.

Significant progress was recently made in describing the aquaporin phosphorylation response to sucrose and salinity.[13,14] Thus, in *Arabidopsis thaliana*, external sucrose addition induced the Ser-282 phosphorylation in PIP2e and therefore a rapid transient opening of pore aquaporin suggesting possibly adjustments to osmotic changes involved in the process.

Also, an absolute quantification procedure was developed to quantify the relative abundance of the unmodified, singly, and diphosphorylated forms of *At*PIP2;1,[14] showing that the *At*PIP2;1 phosphorylation status appears to be highly sensitive to environmental stimuli acting on root water transport, although changes in *At*PIP2;1 phosphorylation were not unequivocally associated to changes in root hydraulic conductivity, Lp_r, and other phosphorylated isoforms and regulatory mechanisms must be considered.

A strategy frequently followed to identify plant PIPs is based on the combination of SDS-PAGE separation of protein extracts followed by western-blot using PIP antibodies. PIPs are characterized by six transmembrane domains; therefore, many commercially available antibodies have been raised against the C-terminal tails of these proteins, which are the most divergent domains among PIPs.[4] Nevertheless, the probable occurrence of PTMs on C-term tails may hurdle the specific identification of PIP isoforms. Alternatively, SDS-PAGE separation of PIP-enriched protein extract combined with endoprotease digestion and subsequent analysis of the peptides by high-performance liquid chromatography coupled to tandem mass spectrometry (HPLC−MS/MS) provides accurate peptide sequence information,[15] which may help to differentiate among PIP isoforms and also enables the characterization of PTMs. The validity of this technique was previously reported by Alexandersson et al.,[16] who identified 238 proteins putatively associated to the plasma membrane using HPLC−MS/MS, including 8 proteins belonging to the PIP family in *A. thaliana*. HPLC−MS/MS is ideally suited for the identification of aquaporins and also allows the characterization of their PTMs.[10,17] Several proteomic studies using *A. thaliana* model organism in combination with HPLC−MS/MS led to the identification of dimethylated and monomethylated forms of *At*PIP2;1.[10] The same technique was used to identify N-terminal Met cleavage in *At*PIP2;1, whereas this residue is N^{α}-acetylated in *At*PIP1;1.[10] HPLC−MS/MS also led to the identification of multiple phosphorylation sites on the N-terminal and C-terminal tails of different plant PIPs.[14,17] Nevertheless, this approach may also have limitations for the study of membrane proteins (including PIPs) because digestion with trypsin, the most frequently used endoprotease, may leave relatively large peptides that can be outside the mass range of the mass spectrometer, or very small peptides (i.e., less than five residues), which may lead to poor identifications after database searches.[18] This is in part due to the distribution of the amino acids Lys and Arg, which are less frequent along integral membrane proteins and almost absent in transmembrane helices. The presence of six trans-membrane segments in PIPs may preclude the steric access of trypsin to Lys and Arg residues near those hydrophobic regions. To try to overcome the limitations of the analysis of PIP proteins after tryptic digestion, previous reports used Lys-C for the analysis and sequencing of aquaporin PM28A.[19] More recently, limited pepsin digestion at lower pH combined with MS/MS analysis allowed the detailed characterization of the integral membrane protein AQP0.[20]

Broccoli, the immature flower vegetable of Brassicaceae (*Brassica oleracea* L. var. italica), is worldwide-known as a health-promoting vegetable because it contains biologically active compounds that serve as chemopreventives of degenerative diseases and certain types of cancer. However, abiotic stresses such as salinization, low water availability and extreme temperatures can severely modify the nutritional quality of this crop. These types of stresses are becoming increasingly important as a consequence of the global reduction in the availability of water resources of good quality for irrigation. In this respect, water and dissolved salts are essential to plant growth, but water reuse and high evaporation rates in arid or semiarid regions such as Southeastern Spain concentrate the salts and salinization occurs. With a gross production over 450 000 tones in 2007, Spain is the major producer and exporter of broccoli in Europe, representing near 20% of the gross production of this crop (http://faostat.fao.org). Together with Spain, broccoli is also grown in Southern areas of Italy and France, where broccoli is grown during the winter season. The economic interest of broccoli as a commodity is coupled to its resistance to relatively cold temperatures and drought as well as salinity. In this case, the control of water and nutrient distribution in the whole plant is an important factor in the acclimation of plants to an unfavorable environment[21] and the role of membrane proteins, such as aquaporins, is crucial. Therefore, the identification of broccoli aquaporin isoforms and their regulation is interesting both from the biochemical and from the agronomical point of view. Despite the socioeconomic value and worldwide trade of broccoli from the standpoint of the plant sciences and also from the Brassicaceae family, the number of nucleotide and amino acid sequences from this species in public databases is very limited (102 nucleotide entries, 2285 ESTs and only 69 complete protein sequences in the NCBI database (http://www.ncbi.nlm.nih.gov)). In this study MS/MS spectra acquired in the linear ion trap were searched against NCBInr and Swiss-Prot databases, including the potential occurrence of modified residues (acetylation, phosphorylation and methylation). Second, MS/MS spectra acquired at high resolution after HCD fragmentation in the Orbitrap were de novo sequenced, in an attempt to find novel peptides not described in protein databases. We found that in those cases where several peptides share the same monoisotopic mass, acquisitions of MS/MS spectra at high resolution followed by database searches helped to discern the presence of a peptide in the sample.

Experimental Procedures

Plant Culture. Seeds of broccoli (*Brassica oleracea* L. var. italica cv. Marathon) were prehydrated with distilled water and continuously aerated for 12 h. After this, the seeds were germinated in vermiculite substrate at 28 °C. Germinated seeds were grown under controlled conditions using a 16 h light followed by 8 h dark cycle and 60% relative humidity at 25 °C. A photosynthetically active radiation (PAR) of 400 μmol m^{-2} s^{-1} was provided by a combination of fluorescent tubes (Philips TLD 36 W/83 and Sylvania F36 W/GRO) and metal halide lamps (Osram HQI, T 400 W). After three days, the seedlings were placed in 15 L containers with a continuous circulation of nutrient solution.[22] Plantlets were harvested after two weeks

and the roots were manually cut and further processed for PIP purification as described below.

Plasma Membrane Protein Purification from Roots and Enzyme Assay. Root plasma membranes were purified using the two-phase aqueous polymer technique first described by Larsson et al.,[23] modified by Gerbeau et al.[24] Fresh roots (20 g) were chopped in approximately 1 mm^3 cubes and vacuum-infiltrated with 40 mL of a buffer containing 500 mM sucrose, 10% glycerol, 20 mM Na_2EDTA, 20 mM EGTA, 50 mM NaF, 5 mM β-glycerophosphate, 1 mM 1,10-phenantroline, 1 mM Na_3VO_4, 0.6% PVP, 5 mM ascorbic acid, 5 mM DTT and 0.5 mg/L leupeptin in 50 mM Tris-MES, pH 8.0. After buffer infiltration, roots were homogenized using pestle and mortar and filtered through a nylon cloth (240 μm pores). The filtrate was centrifuged at 10 000× *g* for 15 min. The supernatant was recovered and centrifuged at 55 000× *g* for 35 min, yielding a microsomal pellet which was resuspended in 0.33 M sucrose, 2 mM DTT, 10 mM NaF and 5 mM phosphate buffer (pH 7.8). Plasma membranes were purified from microsomes by partitioning in a two-phase system mixture with a final composition of PEG-3350 (Sigma)/Dextran-T500 (GE Healthcare), 6.3% (w/w) each in the presence of 5 mM KCl, 330 mM sucrose, 2.5 mM NaF, 5 mM potassium phosphate (pH 7.8) The two phase-system was centrifuged for 5 min at 4000× *g*. The resulting upper phase, enriched in plasma membranes, was washed in 9 mM KCl, 300 mM sucrose, 0.2 M EDTA, 0.2 M EGTA, 0.5 M NaF and 10 mM Tris-borate, pH 8.3, and centrifuged at 55 000× *g* for 35 min; the resulting lower phase was resuspended in 1 mL of 9 mM KCl, 300 mM sucrose, 0.2 M EDTA, 0.2 M EGTA, 0.5 M NaF, 2 mg/L leupeptin, 1 M DTT and 10 mM Tris-borate, pH 8.3. The protein concentration of the PIP-enriched fraction was determined with the RC DC Protein Assay kit (BioRad), using BSA as standard. The purity of the plasma membrane preparation was estimated after measuring the enzymatic activities characteristic of the plasma membrane and other organelles. The activity of the plasma membrane associated, vanadate sensitive ATPase was assayed.[25] The activities of nitrate sensitive ATPase,[26] latent inosine diphosphatase,[27] and cytochrome C oxidase[28] were used as enzymatic markers of tonoplast, Golgi apparatus and mitochondria, respectively. Enzymatic activities were determined in a thermostatted JascoV-530 spectrophotometer (Jasco International Co.) at 25 °C. Extrinsic membrane proteins were stripped with an urea and NaOH treatment[29,30] according to Santoni et al.[18] Briefly, membranes (2 mg proteins) were incubated in 40 mL of 5 mM EDTA, 5 mM EGTA, 4 M urea, 5 mM Tris-HCl, pH 9.5, for 5 min on ice before being centrifuged for 20 min at 100 000× *g*. The subsequent pellet was resuspended in 20 mM NaOH and centrifuged at 100 000× *g* for 20 min. The membranes were then washed in 2 mM EDTA, 2 mM EGTA, 100 mM NaCl, 5 mM Tris-HCl, pH 8, centrifuged at 100 000× *g* for 20 min, and finally resuspended in 9 mM KCl, 300 mM sucrose, 5 mM Na_2EDTA, 5 mM Na_2EGTA, 50 mM NaF, 5 mM dithiothreitol, 2 μg/mL leupeptin, 10 mM Tris-Borate, pH 8.3. The yield of the protein purification procedure, 29%, was calculated by determination of protein concentration after protein solubilization and referred to the amount of initial protein (2 mg).

Gel Electrophoresis and Immunoblotting Assay. A volume of the plasma membrane-enriched preparation corresponding to 50 μg was resolved in a 12% SDS-PAGE gel using a Mini-PROTEAN gel electrophoresis system (Bio-Rad) at 100 V/h. The gel was stained with Bio-Safe Coomassie G-250 (Bio-Rad) for 1 h. Alternatively, 10 μg of the protein extract were resolved in a 12% SDS-PAGE gel as described above and transferred to a PVDF membrane for 20 min at 15 V in an electrophoretic transfer cell (Trans-Blot SD cell, BioRad) using Towbin transfer buffer[31] with the addition of 0.05% SDS. The membrane was blocked for 1 h at room temperature in TBS containing 2% (w/v) skimmed dry milk. After that, the membrane was incubated for 1 h at room temperature in a buffer containing TBS with 0.05% Tween 20 in the presence of an antibody (dilution 1:3000) raised against the first N-terminus 42 residues of *Arabidopsis* PIP1;1[32] (kindly provided by Prof. Dr. Schäffner). Goat anti-rabbit IgG coupled to horseradish peroxidase was used as the secondary antibody (dilution 1:20 000). A chemiluminescent signal was developed using the West-Pico, Super Signal substrate (Pierce).

Endoprotease In-Gel Digestion. The gel bands corresponding to PIPs (monomers and dimers) from three SDS-PAGE gel lanes were excised from the gel and pooled in a single vial, reduced with 10 mM DTT in 25 mM ammonium bicarbonate, S-alkylated cysteine with 55 mM iodoacetamide in 25 mM ammonium bicarbonate and digested with porcine trypsin (Promega) at 37 °C for 6 h as described elsewhere.[33,34] The same procedure was repeated but using Glu-C endoprotease from *Staphylococcus aureus* V8 (Roche). Finally, Lys-C from *Lysobacter enzymogenes* (Roche) was used to digest PIPs as described before but using 25 mM Tris HCl and pH 8.5 as buffer for the digestion. Peptides from the different endoprotease digestions were extracted from the gel slides using acetonitrile (ACN) and 0.1% formic acid. The peptides extracted were transferred to new tubes and dried down under vacuum. The pellets were resuspended in 5 μL of 0.1% formic acid and 5% ACN suitable for HPLC−MS/MS analysis.

Phosphopeptide Enrichment and Analysis. After tryptic digestion, phosphopeptides were enriched using microcolumns packed with TiO_2 beads (Inertsil) as described by Thingholm et al.[35] with few modifications. In short, peptides were resuspended in 5 μL of loading buffer containing 1 M glycolic acid in 80% ACN and 5% trifluoroacetic acid (TFA). The peptides were loaded in the microcolumn with the help of a syringe and washed with 10 μL of wash buffer containing 80% ACN and 5% TFA. Phosphopeptides retained in the microcolumn were eluted with 5 μL of 5% NH_4OH (pH 10.5), dried under vacuum, and finally, resuspended in 5 μL of 0.1% formic acid and 5% ACN suitable for HPLC−MS/MS analysis.

HPLC−MS/MS and Database Searches. HPLC−MS/MS analysis were performed using an Agilent 1200 nano-HPLC (Agilent Technologies) coupled to a LTQ Orbitrap mass spectrometer (Thermo Fisher Scientific) equipped with a nano-ESI source (Proxeon). Peptides were preconcentrated and desalted using Zorbax 300SB-C18 cartridges (5 × 0.3 mm and 5 μm particle size) at 15 μL/min for 10 min in 0.1% formic acid and 5% ACN in water followed by elution on an Zorbax 300SB RP C18 column (75 μm id ×150 mm and 3.5 μm particle size) (Agilent Technologies) using a 60 min linear gradient from 5 to 40% solvent B, solvent A was 0.1% formic acid in water and solvent B was 0.1% formic acid in ACN. All HPLC runs were performed using an Agilent 1200 HPLC system operated at 300 nL/min constant flow rate. The peptides were analyzed in a LTQ Orbitrap mass spectrometer (Thermo Fisher Scientific) equipped with a Proxeon nano-ESI source. An electrospray voltage of 1800 V and a capillary voltage of 50 V at 190 °C were used. The LTQ Orbitrap was operated in data dependent mode as follows: survey scans (400−2000 m/z) were acquired at 60 000 full width at half-maximum (fwhm) resolution at m/z 400 followed by

Table 1. Enzymatic Activities (nmol min^{-1} mg^{-1} Protein) of Plasma Membrane and Microsomal Fractions Measured in the Supernatant of the PIP Purification after Two-Phase Extraction Method[a]

		nmol min^{-1} mg^{-1} protein		
enzyme	organelle	PM fraction	rest of organelles fraction	percentage (%) of the enzyme activity in the PM fraction
vanadate-sensitive ATPase	plasma membrane	200 ± 22.2	10 ± 1.2	95.2
nitrate-sensitive ATPase	tonoplast	15 ± 3.2	300 ± 33.2	4.8
citrochrome C oxidase	mitochondria	50 ± 7.9	1508 ± 101.2	3.2
inosine diphosphatase	Golgi apparatus	1.3 ± 0.5	37 ± 8.2	3.4

[a] Measurements were carried out in the plasma membrane enriched fraction and in the microsomal fraction. Data are mean ± SE of five replications.

CID fragmentation of the six most intense peaks at 35% normalized collision energy and scanned in the linear ion trap. Maximum injection time for MS and MS/MS were set to 50 and 500 ms, respectively. The precursor isolation was 2 Da and the exclusion mass width was set to ±5 ppm. Monoisotopic precursor selection was allowed and singly charged species were excluded. The minimum intensity threshold for MS/MS was 1000 counts for the linear ion trap and 8000 counts for the Orbitrap. Maximal ion accumulation time allowed on the LTQ Orbitrap was 50 ms for MS and 500 ms for MS/MS. Automatic gain control (AGC) to prevent overfilling of the ion trap were set as follows: 5×10^5 for Orbitrap MS and 1×10^5 for Orbitrap MS/MS.

The following parameters were set for searches using Proteome Discoverer v.1.1 (Thermo Fisher Scientific) and SEQUEST[36] as search engine: Precursor ion tolerance of ±10 ppm and fragment ion tolerance of ±0.5 Da were allowed, unless otherwise stated. The number of missed cleavages allowed was 2 in every case. Fixed modifications: carboxyamidomethyl Cys; variable modifications: oxidation of Met, N-terminal acetylation (+42.011 amu), Ser phosphorylation (+79.966 amu), Lys and Glu methylation (+14.016 amu); Lys dimethylation (+28.031 amu); Lys trimethylation (+42.047 amu). All fragmentation spectra were searched against NCBInr (8 921 653 entries) and Swiss-Prot v. 57.4 (470 369 entries) databases available at (ftp://ftp.ncbi.nih.gov/blast/db/FASTA). A ≤5% peptide false discovery rate (FDR) filter was set for the searches against reversed-concatenated databases. Independent searches against both, NCBInr and Swiss-Prot databases were carried out selecting the three endoproteases: trypsin, Lys-C and Glu-C in Proteome Discoverer v.1.1 search engine.

De Novo Sequencing. For *de novo* sequencing, the LTQ Orbitrap was operated in data dependent mode as follows: survey scans (400−2000 m/z) were acquired at 60 000 fwhm resolution at m/z 400 followed by three Data Dependent HCD MS/MS scans (100−2000 m/z), with 7500 fwhm resolution at m/z 400. Normalized collision energy used for HCD fragmentation was 40%. The rest of the variables were set as described above. MS/MS spectra acquired were submitted to *de novo* sequencing using PEAKS v4.5 SP2 software (www.bioinformaticssolutions.com). Parental and fragment mass error tolerances were ±5 ppm and ±0.005 Da, respectively. Only those peptide sequences with Peaks scores ≥75 and with at least four amino acids with confidence 99.5 were considered as *de novo* sequenced peptides. Raw files acquired after HCD MS/MS as described above were also used for database searches when higher mass accuracy of fragment ions was needed.

Sequence Alignment and Transmembrane Modeling. Multiple sequence alignment of PIPs sequences and the peptides identified in our experiments was carried out with ClustalW.[37]

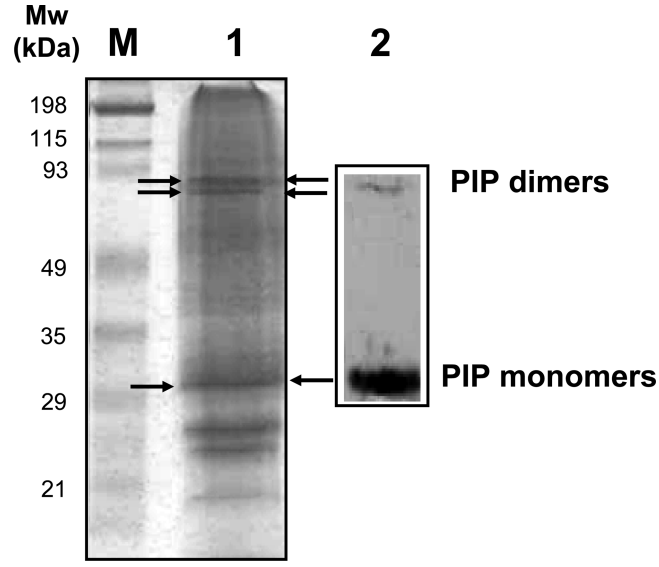

Figure 1. Enrichment of PIP aquaporins extracted from broccoli roots by the two-phase aqueous polymer technique. (M) Molecular weight marker. (1) Volume of supernatant corresponding to 50 μg of purified proteins was analyzed by 12% SDS-PAGE and stained with Coomassie Brilliant Blue. (2) Western-blot using PIP1 antibody. PIP1 was raised against the 42 N-terminal residues of PIP1;1 from *A. thaliana*. Goat antirabbit IgG coupled to horseradish peroxidase was used as the secondary antibody (1:20000). Protein Molecular weight markers (M_w) are also shown (kDa).

Predicted transmembrane regions were identified using TMHMM[38] and "re-entrant" loops were predicted with TMLoop software.[39]

Results and Discussion

Membrane Protein Purification. The protocol used here, combining the two-phase aqueous polymer technique method followed by urea-NaOH treatment,[18,40] yielded a protein preparation specifically enriched in plasma membrane intrinsic proteins, with less than 5% contamination of other membrane organelles (Table 1). As shown in this table, the specific vanadate sensitive ATPase activity was 95.2% ($n = 4$). Tonoplast, Golgi apparatus and mitochondria contaminations accounted for 4.8, 3.4, and 3.2% of the total ATPase activity, respectively ($n = 4$).

As displayed in the gel in Figure 1, both the SDS-PAGE gel and the western-blot revealed the presence of a lower band of ca. 30 kDa, corresponding to the monomeric form of PIPs. Two upper bands of 61 and 63 kDa were also detected, corresponding to dimeric forms of PIPs. The visualization of the upper band at 63 kDa, approximately 2 kDa bigger than the dimeric form of PIPs at 61 kDa, suggests the occurrence of dimeric PIPs

bearing relatively heavy PTMs such as glycosylated or ubiquitinated branches. Although not described for plants, several aquaporins containing N-linked glycosylation,[41,42] and ubiquitination[43,44] have been reported. These two modifications intervene in the regulation and degradation of aquaporins in mammals.[41−45] The occurrence of glycosylation and ubiquitination on plant aquaporins can not be discarded, although the characterization of these two PTMs is beyond the scope of this study.

Unlike other known aquaporins, broccoli PIP dimers were not dissociated after treatment with 2% SDS, high temperature (56 °C for 20 min), chaotropic agents (8 M urea or 6 M guanidinium chloride), or reducing agents (140 mM β-mercaptoethanol or 100 mM DTT). This strong multimeric aquaporin association was also described for *Escherichia coli* aquaporin AqpZ, where stable tetramers were found that were not readily dissociated by 1% SDS.[46] It was not possible to resolve the purified PIP proteins by 2D-PAGE (data not shown), probably due to their high hydrophobicity, which agrees with previous reports focusing on PIP protein analysis from culture cell suspensions from *Arabidopsis*[47] and rice.[48]

The validity of the membrane protein purification protocol described here directly from plant roots was confirmed by the identification, together with our proteins of interest, of peptides homologous to those found in plasma membrane ATPase 2 (PMA2_ARATH), ATPase 9 (PMA9_ARATH) and ATPase 10 (PMA10_ARATH), calcium transporting ATPase 2 (ACA2_ARATH) and sugar transporter protein 1 (STP1_ARATH), after database search (see Supplementary excel files in the Supporting Information). All these transmembrane proteins contain, at least, 10 transmembrane domains, according to modeling algorithms based on their amino acid sequence.

Identification of PIP Peptides after Endoprotease Digestion. To identify the presence of PIP proteins in broccoli roots, we carried out independent digestion and analysis of the PIP gel bands using three endoproteases (trypsin, Lys-C and Glu-C). As described above in the introduction, trypsin and Lys-C were successfully used for the characterization of aquaporins. We also introduced the use of Glu-C based on the observation that *At*PIPs include a relatively high number of Glu and Asp residues. The peptides derived after each endoprotease digestion were analyzed by HPLC−MS/MS, which led to the successful identification of 23 peptides corresponding to PIPs after CID fragmentation and detection of fragment ions in the linear ion trap analyzer (Table 2). The majority of the peptides identified corresponded to tryptic peptides, followed by Lys-C. Only one peptide was uniquely identified after Lys-C digestion. As shown in Table 2, some of the peptides identified by SEQUEST after database search were attributed to different PIP isoforms within the same species or even to PIPs from different plant species. As an example, the peptide SFGAAVIYNNEK can be assigned to PIP2;4, PIP2;7 or PIP2;8 isoforms from *Arabidopsis thaliana*. Another example is the peptide DVEGAEGVTAR, which could be assigned to both PIP2 from *Brassica napus* and PIP2;3 from *Raphanus sativus*. Peptides corresponding to both PIP1 and PIP2 subclasses and from different plant species were detected, including those from the Brassicaceae family (*Brassica napus*, *Raphanus sativus*, *Brassica oleracea*, *Thlaspi caerulescens*, *Brassica campestris*, and *Arabidopsis thaliana*) and also from *Petunia hybrida*, from the Solanaceae family.

In an attempt to clarify these inconsistencies found after database searches, we decided to include a column showing the attribution of each peptide identified in our experiments to the homologue sequence described in *A. thaliana* and, eventually, the corresponding isoforms. All the peptides identified showed relatively high degree of sequence homology to *A. thaliana* PIP sequences, as derived from BlastP scores, ranging from 32.9 to 74.0.[49]

The majority of the peptides identified showed negative grand average hydrophobicity (GRAVY) values,[50] indicating a relatively high hydrophilicity. However, the peptides SLGAAIIFNK and SLGAAIIYNK shared a sequence that corresponds to a transmembrane region (shown underlined) and displayed hydrophobic GRAVY values of +1.060 and +0.650, respectively. The identification of these hydrophobic transmembrane peptides could be explained based on previous reports focusing on the characterization of membrane proteins stating that denatured membrane proteins in the SDS-PAGE gel matrix may increase the steric access of endoproteases, thus improving the identification of peptides from this recalcitrant proteins.[51]

Characterization of Post-Translational Modifications. Several post-translational modifications were detected on peptides from PIPs isolated from broccoli roots, including acetylation, phosphorylation and methylation. Acetylation on the N-terminal Met of PIPs was detected, as derived from the identification of two peptides with sequence M_{ac}EGKEEDVR and M_{ac}EGKEEDVRVGANK (Table 2). The second peptide shares a sequence of nine residues with the first peptide (underlined), and was identified as a consequence of the occurrence of a missed cleavage site for trypsin and also after the HPLC−MS/MS analysis of the digestion with Lys-C. All these peptides identified correspond to the PIP1 subclass of PIPs and confirm the presence of N-terminal acetylation on PIP1 proteins in broccoli. An example of a MS/MS spectrum showing the identification of the peptide M_{ac}EGKEEDVR at m/z 567.760 Da is shown in Figure 2A. The presence of N-terminal acetylated Met on PIP1 agrees with previous reports on PIP characterization by MS.[10] Enzymatic acetylation of the N-terminus of proteins by acetyl transferases occurs in about 50% of yeast proteins, and up to 90% of higher eukaryotic proteins.[52−54] Acetylation can occur on the N-terminal Met by methionine aminopeptidases (MAPs).[53,54] MAPs can also cleave N-terminal methionyl residues and acetylate the second amino acid when the second residue on the growing protein is small (i.e., Gly, Ala, Ser, Cys, Thr, Pro, and Val).[55] A variant of N-terminal acetylation, in which the N-terminal Met-Glu sequence is N-acetylated, is also frequently observed.[56] According to our results, acetylation of PIP1 found in broccoli occurs before the initial Met is cleaved by MAPs. The identification of acetylated N-terminal Met-Glu motif suggest the presence of an enzyme similar to N-acetyl transferase B (NatB) from yeast, able to acetylate most of the proteins with Met-Asp or Met-Glu N-termini.[54] Nevertheless, the biological significance of N-terminal acetylation of eukaryotic proteins still remains unclear.

We included the potential occurrence of phosphorylation on Ser and Thr in all database searches, which led to the identification of two different phospho-Ser residues localized near the C-term of PIP2 (SLGSFRS_pAANV and SLGS_pFRSAANV at m/z 594.776). Further analysis including the enrichment of phosphopeptides using TiO_2 microcolumns (see Experimental Procedures) followed by HPLC−MS/MS analysis led to the unambiguous identification of the doubly phosphorylated form of this peptide with sequence SLGSpFRSpAANV at m/z 634.757) (Table 2 and Supplementary Files 7 and 8, Supporting Information). As depicted in Figure 2B, the presence of the two

Table 2. List of Aquaporin Peptides Identified in the Plasma Membrane of Broccoli Roots after Database Search[a]

peptide sequence/endoprotease[b]	MH^+ NCBI/Swiss-Prot[c]	Δ mass (ppm) NCBI/Swiss-Prot[d]	isoform	species[e]	homologue sequence in *Arabidopsis thaliana*/ISOFORM	BlastP score
AFQSAYYVR/T	1104.550/n.d.	2.650/n.d.	PIP2	*Brassica napus*	A^{144}FQSAYFTR^{152}/PIP2;5	32.9
			PIP2;3	*Raphanus sativus*		
DVEAVSGEGFQTR/T/Ti	1394.658/n.d.	2.530/n.d.	PIP1	*Brassica napus*	D^{4}VEAVPGEGFQTR^{16}/PIP2;1	43.1
			PIP2	*Raphanus sativus*		
DVEGAEGVTAR/T	1103.536/n.d.	3.606/n.d.	PIP2	*Brassica napus*	D^{4}VEGPEGFQTR^{14}/PIP2;2	35.8
			PIP2;3	*Raphanus sativus*		
DVRVGANKFPE/G	1231.644/1231.644	1.220/1.220	Aquaporin	*Brassica napus*	D^{7}VRVGANKFPER^{18}/PIP1;1, 1;2, 1;3, 1;4, 1;5	38.0
			Aquaporin	*Brassica juncea*		
			Aquaporin	*Brasita rapa*		
			PIP1	*Thlaspi caerulescens*		
			PIP1b1, PIP1b2	*Brassica oleracea*		
			PIP1;2, PIP1;3	*Raphanus sativus*		
			PIP1;1, 1;2, 1;3, 1;4, 1;5	*Arabidopsis thaliana*		
DYEDPPPTPFFDADEmeLTK/T/Ti	2110.955/2110.955	2.782/2.782	PIP2;2	*Arabidopsis thaliana*	D^{15}YEDPPPTPFFDADELTK^{32}/PIP2;2	63.4
DYEDPPPTPFFDAEELTK/T/Ti	2110.955/2110.955	2.782/2.782	PIP2;2	*Raphanus sativus*	D^{15}YEDPPPTPFFDAEELTK^{32}/PIP2;3	63.4
			PIP2;3	*Raphanus sativus*		
			PIP2	*Brassica napus*		
			PIP2;3	*Arabidopsis thaliana*		
FPERQPIGTSAQSDK/L	1660.833/1660.833	1.419/1.419	PIP1;2, PIP1;3	*Raphanus sativus*	F^{15}PERQPIGTSAQSDK^{29}/PIP1;1, 1;2	50.3
			PIP1b1, PIP1b2	*Brassica oleracea*		
			Aquaporin	*Brassica juncea*		
			Aquaporin	*Brassica napus*		
			PIP1	*Thlaspi caerulescens*		
			PIP1;1, 1;2	*Arabidopsis thaliana*		
FPERQPIGTSAQTDK/L	1674.847/n.d.	1.822/n.d.	PIP1;2, PIP1;3	*Raphanus sativus*	F^{15}PERQPIGTSAQTDK^{29}/PIP1;3	50.7
			PIP1b1, PIP1b2	*Brassica oleracea*		
			Aquaporin	*Brassica juncea*		
			Aquaporin	*Brassica napus*		
			PIP1	*Thlaspi caerulescens*		
			PIP1;3	*Arabidopsis thaliana*		
GFQPKmeQYQALGGGANTVAPGYTK/T	2367.203/n.d.	−2.262/n.d.	PIP1;2, PIP1;3	*Raphanus sativus*	Q^{157}YQALGGGANTVAHGYTK^{174}/PIP1;1	74.0
			Aquaporin	*Brassica oleracea*		
			Aquaporin	*Brassica campestris*		
			Aquaporin	*Brassica napus*		
			PIP1	*Thlaspi caerulescens*		
GFQPTPYQTLGGGANTVAPGYSK/T	2311.142/n.d.	3.011/n.d.	Aquaporin	*Brassica juncea*	G^{150}FQPTPYQTLGGGANTVAHGYTK^{174}/PIP1;4	74.0
QYQALGGGANTVAHGYTK/T	1835.908/1835.906	2.698/1.634	PIP1b1, PIP1b2 PIP	*Brassica oleracea*	Q^{157}YQALGGGANTVAHGYTK^{174}/PIP1;1	58.3
			PIP	*Raphanus sativus*		
			PIP1;1	*Arabidopsis thaliana*		
QYQALGGGANTVAPGYTK/T/L	1795.903/n.d.	3.390/n.d.	PIP1;2, PIP1;3	*Raphanus sativus*	Q^{157}YQALGGGANTVAHGYTK^{174}/PIP1;1	57.9
			Aquaporin	*Brassica oleracea*		
			Aquaporin	*Brassica campestris*		
			Aquaporin	*Brassica napus*		
			PIP1	*Thlaspi caerulescens*		

Table 2. Continued

peptide sequence/endoprotease[b]	MH$^+$ NCBI/Swiss-Prot[c]	Δ mass (ppm) NCBI/Swiss-Prot[d]	isoform	species[e]	homologue sequence in *Arabidopsis thaliana*/ISOFORM	BlastP score
MacEGKEEDVR/T	n.d./1134.512	n.d./2.420	PIP1b1, PIP1b2	*Brassica oleracea*	M^{1}EGKEEDVR^{9}/PIP1;1, 1;2, 1;3, 1;4	33.3
			PIP1;2, PIP1	*Raphanus sativus*		
			PIP1	*Thlaspi caerulescens*		
			PIP1;1, 1;2, 1;3, 1;4	*Arabidopsis thaliana*		
MacEGKEEDVRVGANK/L	n.d./1603.778	n.d./2.158	PIP1b1, PIP1b2	*Brassica oleracea*	M^{1}EGKEEDVRVGANK^{14}/PIP1;1, 1;2, 1;3, 1;4	47.7
			PIP1;2, PIP1;3	*Raphanus sativus*		
			Aquaporin	*Brassica juncea*		
			Aquaporin	*Brassica rapa*		
			PIP1	*Thlaspi caerulescens*		
			PIP1;1, 1;2, 1;3, 1;4	*Arabidopsis thaliana*		
SFGAAVIYNNEK/T	1312.656/1312.656	2.700/2.700	Aquaporin	*Brassica oleracea*	S^{225}FGAAVIYNNEK^{236}/PIP2;4, 2;7, 2;8	40.9
			PIP2;4, 2;7, 2;8	*Arabidopsis thaliana*		
SFGAAVIYNQDK/T	1312.657/n.d.	2.886/n.d.	PIP2;2	*Petunia hybrida*	S^{225}FGAAVIYNNEK^{236}/PIP2;4, 2;7, 2;8	40.9
SFGAAIIFNK/T	1033.607/1033.607	3.485/3.485	PIP1;2, PIP1;3	*Raphanus sativus*	S^{239}LGAAIIFNK^{248}/PIP1;3	33.3
			PIP1b1, PIP1b2	*Brassica oleracea*		
			Aquaporin	*Brassica napus*		
			Aquaporin	*Brassica campestris*		
			PIP1	*Thlaspi caerulescen*		
			PIP1;2	*Arabidopsis thaliana s*		
SLGAAIIYNK/T	1049.599/1049.601	0.498/2.243	PIP1;1	*Raphanus sativus*	S^{231}LGAAIIYNKDK^{242}/PIP1;1, 1;3, 1;4, 1;5, PIP2;5	33.7
			PIP1;1, 1;3, 1;4, 1;5, PIP2;5	*Arabidopsis thaliana*		
SLGSpFRSAANV/T/L	1188.543/1188.543	2.266/2.266	PIP1, PIP2	*Brassica napus*	S^{277}LGSFRSAANV^{287}/PIP2;1, 2;2, 2;3	35.0
			PIP2;2, PIP2;3	*Raphanus sativus*		
			PIP2;1, 2;2, 2;3	*Arabidopsis thaliana*		
SLGSFRSpAANV/T	1188.543/1188.543	2.266/2.266	PIP1, PIP2	*Brassica napus*	S^{277}LGSFRSAANV^{287}/PIP2;1−2;2−2;3	35.0
			PIP2;2, PIP2;3	*Raphanus sativus*		
				Arabidopsis thaliana		
SLGSpFRSpAANV/T/Ti	n.d./1268.508	n.d./0.759	PIP1, PIP2	*Brassica napus*	S^{277}LGSFRSAANV^{287}/PIP2;1, 2;2, 2;3	35.0
			PIP2;2, PIP2;3	*Raphanus sativus*		
			PIP2;1, 2;2, 2;3	*Arabidopsis thaliana*		
TPYNTLGGGANTVAPGYSK/T/L	1867.922/n.d.	1.946/n.d.	Aquaporin	*Brassica oleracea*	T^{142}PYNTLGGGANTVADGYSK^{160}/PIP2;7	60.9
VGANKFPER/T	1017.551/1017.551	3.892/3.292	PIP1b1, PIP1b2	*Brassica oleracea*	V^{10}GANKFPER^{18}/PIP1;1, 1;2, 1;3, 1;4, 1;5	31.6
			PIP1;2, PIP1;3	*Raphanus sativus*		
			Aquaporin	*Brassica campestris*		
			Aquaporin	*Brassica napus*		
			PIP1	*Thlaspi caerulescens*		
			PIP1;1, 1;2, 1;3, 1;4, 1;	*Arabidopsis thaliana*		

[a] Occurrence of acetylation (ac), methylation (me) and phosphorylation (p) is indicated. [b] Endoprotease used for in-gel digestion: trypsin: T, Glu-C: G, Lys-C: L, peptide detected after enrichment with TiO_2: Ti. [c] Monoisotopic mass of the singly charged peptide $[M + H]^+$. [d] Mass difference (Δ mass) between experimental and theoretical monoisotopic masses or the precursor ions. n.d. is the abbreviation for not detected. [e] Species from the Brasiccaceae family whose peptides share 100% sequence homology with peptides identified in *Brassica oleracea* var. Italica roots, as derived after BlastP algorithm.

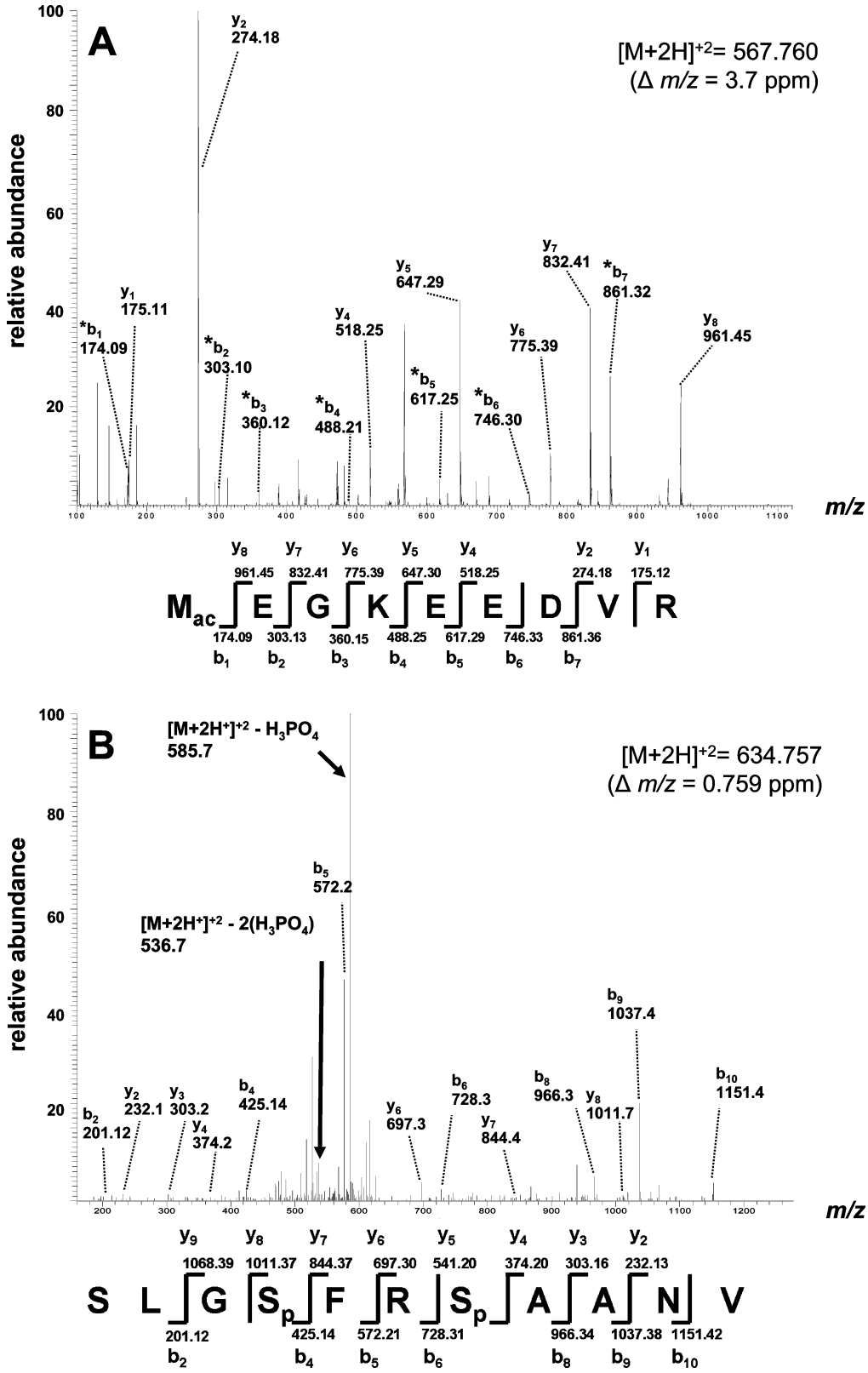

Figure 2. Identification of PIP acetylation (ac) and phosphorylation (p) by mass spectrometry. (A) MS/MS fragment spectra corresponding to the N-terminal acetylated tryptic peptide M_{ac}EGKEEDVR (m/z = 567.760). (B) MS/MS fragment spectra corresponding to the C-terminal doubly phosphorylated peptide $SLGS_pFRS_pAANV$ (m/z = 634.757). The presence of the double phosphorylation is supported by the observation of two neutral losses of phosphoric acid from the precursor ion (−49.0 and −98.0 Da), indicated with arrows. Diagnostic fragment ions (*y* and *b*) bearing the phosphate are indicated with (*). The monoisotopic masses of the doubly charged species detected and the delta masses (Δ m/z) in parts per million (ppm) are indicated. The peptide sequences and the assigned fragment ions are indicated. The expected ion masses are also listed above the sequence.

phosphate moieties on this peptide was confirmed by the presence of two neutral losses in the MS/MS spectrum, the first at −49 Da ($[M + 2H]^{+2}$-H_3PO_4) and the second at −98 Da corresponding to the loss of two phosphoric acid molecules ($[M + 2H]^{+2}$-$2(H_3PO_4)$). Neutral losses are frequently observed after fragmentation of peptides containing phosphorylated Ser and/or Thr residues[19,33] and, together with the mass of the precursor ion, serve to confirm the occurrence of phosphate moieties. Interestingly, although phosphopeptide enrichment using TiO_2 seems to show a bias toward monophosphorylated peptides,[56] only this purification led to the identification of the doubly phosphorylated peptide from PIP2. We would like to underline that, in all our experiments, the phosphopeptide always contained one trypsin missed cleavage site (R), which is in agreement with previous reports by Molina et al.,[57] who showed that the frequency of tryptic missed cleavages sites is significantly higher for phosphorylated peptides. We could not detect the unphosphorylated form of the peptide with sequence SLGSFRSAANV in any of our analyses. This could be due to the confinement of this peptide species into the acrylamide gel after digestion or, more probably, to the majority presence of the phosphorylated versus the unphosphorylated peptide in the sample under study. On the other hand, several non-phosphorylated peptides containing at least three acidic residues were also identified after the enrichment with TiO_2 microcolumns. This is in agreement with previous reports showing the ability of TiO_2 to bind acidic peptides.[56,58,59] The identification of acidic peptides after TiO_2 enrichment served as a confirmation of the occurrence of those peptides in our PIP-enriched protein purification (indicated by "Ti" in Table 2).

In general, mammalian, yeast and plant aquaporins N- and C-terminal tails have been predicted to be fairly mobile, as derived from structural studies.[60−63] Therefore, PIPs C- and N-tails have been proposed to intervene in the protein channel gating which, in turn, regulates water flow.[12,20,64,65] The last is supported by structural data from yeast aquaporin Aqy1, which showed that the N-terminus of this aquaporin has a functional role in the gating of the membrane channel.[63] Focusing on PIPs, the determination of spinach *So*PIP2;1 structure at atomic resolution proposed that, in the closed conformation, the second cytoplasmic loop D of this protein occludes the protein channel.[64]

In the case of plants, it has been proposed that PIPs channel gating is probably regulated upon phosphorylation of residues near the C-terminal tails.[12,20,66] Conversely, the only mammalian aquaporin reported to be gated by phosphorylation on Ser^{111} (inside the B-loop) is human AQP4 from astrocytes, which plays a key role for maintenance of brain water homeostasis.[67] The hypothesis of plant PIP regulation upon phosphorylation on C-tails is supported by the fact that site-directed mutagenesis experiments have suggested that Ser-phosphorylation may intervene in the regulation of PIPs water transport activity.[20,68−71] Recently, Prak et al[14] demonstrated that the C-terminal *At*PIP2 phosphorylation pattern changed as a consequence of changes of NaCl concentration in the nutrient solution or exposure to H_2O_2 using the absolute quantification (AQUA) strategy[72] and correlated the changes in the global phosphorylation pattern of PIPs with altered root water transport activity. Moreover, *A. thaliana* PIPs present multiple and interdependent phosphorylation sites on their C-terminal tails, meaning that phosphorylation on specific residues strongly promote phosphorylation on nearby residues inside the same protein.[14,18,20,73] As an example, interdependent phosphorylation on Ser^{280} and Ser^{283} on the C-terminal tail of *At*PIP2 has been demonstrated.[14,74] The identification of phosphopeptides ($SLGS_pFRSAANV$, $SLGSFRS_pAANV$ and $SLGS_pFRS_pAANV$) suggests that phosphorylation of the C-terminus of PIPs may be involved in the regulation of water uptake in broccoli roots.

Two peptides with sequences $GFQPK_{me}QYQALGGGANTVAPGYTK$ and $DYEDPPPTPFFDADE_{me}LTK$ were found to be methylated on Lys and Glu, respectively (Table 2). Focusing on the second methylated peptide, as shown in Table 2, database search lead to the identification of two different peptides (i.e., DYEDPPPTPFFDA<u>E</u>ELTK and DYEDPPPTPFFDA-<u>D</u>E_{me}LTK) sharing the same monoisotopic mass at MH^+= 2110.955 and charge state ($z = 2$) after measurement of the precursor ion in the Orbitrap analyzer. These two peptides only differed in one acidic amino acid residue (shown underlined) and both occur in different PIP isoforms (i.e., PIP2;3 and PIP2;2, respectively) in *A. thaliana*. In an attempt to confirm the presence of both peptides in our sample, we repeated the analysis measuring both, precursor ion and fragment ions in the Orbitrap analyzer after HCD fragmentation and using more stringent tolerances for the search of fragment ions (±0.005 Da instead of the ±0.5 Da allowed for fragment ions measured in the linear ion trap). This strategy led to the identification of only the nonmethylated peptide (Supplementary Table 1, Supporting Information). Figure 3 shows fragment spectra corresponding to the methylated peptide DYEDPPPTPFFDA-<u>D</u>E_{me}LTK after CID fragmentation (Figure 3A) and nonmethylated peptide (DYEDPPPTPFFDA<u>E</u>ELTK after CID and HCD fragmentation (Figure 3B and C). In Figure 3A and B, the MS/MS fragment spectra after CID fragmentation of these two peptides detected in the linear ion trap, methylated and nonmethylated, showed that only four fragment ions (y_4, y_5, b_{13} and b_{14}) varied when the two fragmentations were compared, which could lead to the unambiguous identification of the presence/absence of methylation. Only y_4 and y_5 were identified in the methylated peptide (Figure 3A), and the four diagnostic fragment ions were identified in the nonmethylated peptide (Figure 3B) using the same precursor and fragment mass error tolerance. The detection of the nonmethylated peptide (DYEDPPPTPFFDA<u>E</u>ELTK) was confirmed after HCD fragmentation and detection of fragment ions in the Orbitrap analyzer after database search using more stringent tolerances for database search (±0.005 Da) (Figure 3C). This peptide, evidenced the presence of PIP2;3, as it is exclusively found in this PIP isoform.

Nevertheless, the presence of O-methylated Glu and N-methylated Lys on the N-terminus of PIP2 has been confirmed in previous publications.[6,10] However, the peptide $DYEDPPPTPFFDADE_{me}LTK$ indicating the methylation of PIP2;2 in the roots of broccoli plants differed in the methylated peptide (AKDVEGPEGFQTR) of the PIP2;2 isoform from *Arabidopsis*, and the methylation in $GFQPK_{me}QYQALGGGANTVAPGYTK$ supported to our knowledge the first evidence of methylation in the C-terminus of PIP1 in plants. The cited studies[6,10] also show that methylation on Glu and Lys does not interfere PIP water permeability and suggest that aquaporin methylation could be involved in protein stability and subcellular localization. For this reason, the presence of the Glu-methylated peptide can not be ruled out and should be further validated using independent experiments such as western-blot or site directed mutagenesis.[10]

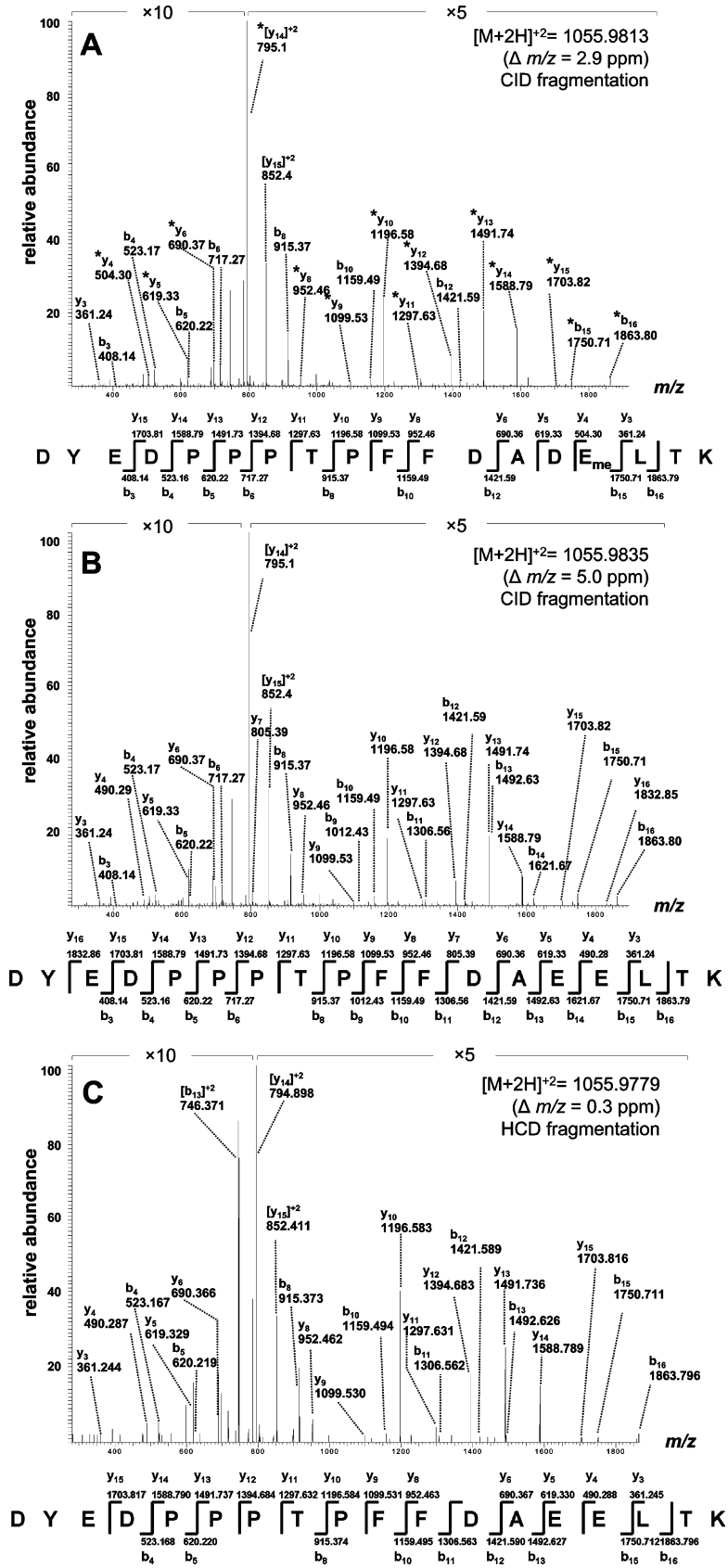

Figure 3. Analysis of PIP methylation (me) by mass spectrometry combining collision induced dissociation (CID) and higher-energy C-trap dissociation (HCD) types of fragmentation. (A) MS/MS fragment spectra after CID corresponding to a potential methylated tryptic peptide DYEDPPPTPFFDADE$_{me}$LTK (m/z = 1055.9813). Diagnostic fragment ions (y and b) bearing the methylation are indicated with (*). (B) MS/MS fragment spectra after CID corresponding to the peptide D^{15}YEDPPPTPFFDAEELTK^{32} (m/z = 1055.9835). (C) MS/MS fragment spectra after HCD corresponding to the peptide D^{15}YEDPPPTPFFDAEELTK^{32} (m/z = 1055.9835). The peptide sequence and the assigned fragment ions are indicated. The expected ion masses have been listed above the sequence.

Table 3. *De Novo* Sequenced Peptides Identified in the 30 kDa and 60 kDa Bands of the Plasma Membrane Proteins Fraction of Broccoli Roots[a]

m/*z*	*z*	MH^{+b}	peptide sequence	homologue sequence in *Arabidopsis thaliana*/position inside sequence[c]	peaks score (%)[d]	isoforms/species [e]
560.7700	2	1120.542	AFQSSYY**V**R	A^{145}FQSSYYTR^{153} (PIP2;1,PIP2;2,PIP2;3,PIP2;4)/loop C	99.97	PIP1/*Brassica napus* PIP2;2/*Raphanus sativus*
552.7800	2	1104.547	AFQSAY**YV**R	A^{144}FQSAYFTR^{152} (PIP2;5)/loop C	98.70	PIP2/*Brassica napus* PIP2;3/*Raphanus sativus*
656.8300	2	1312.653	SFGAAV(I/L)YNNEK	S^{225}FGAAVIYNNEK^{236} (PIP2;4,PIP2;7,PIP 2;8)/ transmembrane-loop E	98.58	Aquaporin/*Brassica oleracea*
509.2800	2	1017.548	VGANKFPER	V^{10}GANKFPER^{18} (PIP1;1,PIP1;2, PIP1;3, PIP1;4, PIP1;5)/N-terminus	94.65	Putative aquaporin/*Brassica napus* Aquaporin/*Brassica campestris* PIP1b1, PIP1b2/*Brassica oleracea* PIP1/*Thlaspi caerulescens* PIP1;2, PIP1;3/*Raphanus sativus*
459.7400	2	918.479	**Q**NKFPER	A^{12}NKFPER^{18} (PIP1;1, PIP1;2, PIP1;3, PIP1;4, PIP1;5)/N-terminus	95.76	Putative aquaporin/*Brassica napus* Aquaporin/*Brassica campestris* PIP1b1, PIP1b2/*Brassica oleracea* PIP1/*Thlaspi caerulescens* PIP1;2, PIP1;3/*Raphanus sativus*
531.9300	3	1593.781	**WWAVAV**SGEGFQTR	A^{7}VPGEGFQTR^{16} (PIP2;1)/N-terminus	98.39	PIP1/*Brassica napus* PIP2;1/*Raphanus sativus*
531.9300	3	1593.781	**WQW(I/L)**VSGEGFQTR	A^{7}VPGEGFQTR^{16} (PIP2;1)/N-terminus	93.21	PIP1/*Brassica napus* PIP2;1/*Raphanus sativus*
898.4500	2	1795.897	QYQALGGGANTVA**P**GYTK	Q^{157}YQALGGGANTVAHGYTK^{174} (PIP1;1)/loop C	83.79	PIP1;2/*Raphanus sativus* PIP1;3/*Raphanus sativus* PIP1b2/*Brassica oleraceae* Aquaporin/*Brassica campestris* Putative aquaporin/*Brassica napus* PIP1/*Thlaspi caerulescens*

[a] Bold characters indicate the amino acid residues differing from *Arabidopsis thaliana* sequence. (I/L) denotes the impossibility to distinguish the occurrence of Ile or Leu in a given position inside the peptide. [b] **MH**$^{+}$ values were calculated using Peptide Mass Calculator v3.2 available at http://rna.rega.kuleuven.ac.be/masspec/pepcalc.htm, selecting N-term free amine and C-term acid. [c] The position of the residues inside the homologue sequences in *A. thaliana* is indicated with superscript numbers. [d] Peaks score: probability score derived by Peaks v.4.5 search algorithm. [e] Species from the Brasiccaceae family whose peptides share 100% homology with the peptide sequences from the roots of *Brassica oleracea* var. Italica. as derived after BlastP algorithm.

De Novo Sequencing of PIPs. In an attempt to further characterize peptides not identified after database searches, the unassigned spectra were submitted to *de novo* sequencing using Peaks v4.5 algorithm. After the measurement of a peptide precursor ion *m*/*z*, charge state and MS/MS fragments, it is possible to reconstitute the sequence of a peptide by comparing mass differences between consecutive pairs of *b* and *y* ions with the masses of amino acid residues. This process is known as *de novo* peptide sequencing, and it is independent of any information present in databases. Although *de novo* sequencing can be carried out by manual interpretation of the spectra, today there is the possibility of interpreting peptide fragmentations with the help of dedicated computer programs[75,76] especially if the masses of precursor and fragment ions are measured accurately and with high resolution.

We identified eight peptide sequences after the analysis of tryptic peptides by HPLC−MS/MS measuring the masses of precursor and fragment ions in the Orbitrap analyzer and *de novo* sequencing. These peptide sequences are shown in Table 3. Seven of the eight peptides identified after *de novo* sequencing differed in, at least, one amino acid from the homologue peptides in *A. thaliana* (bold characters in Table 3). The eight peptides displayed a high homology to PIP sequences from the Brassicaceae family after BlastP[49] searches against NCBInr database. The alignment of the *de novo* sequenced peptides showed that five of eight peptides sequenced corresponded to the PIP2 subfamily whereas three of them corresponded to the PIP1 subfamily. An example of a peptide *de novo* sequenced that could not be found after database search is shown in Figure 4. A detailed view of the low *m*/*z* region of the MS/MS spectra of this peptide showed the presence of the y_1 fragment corresponding to R at the C-terminus and the presence of diagnostic ions for E (102.05), F (120.08) and W (130.05 and 159.09). The partial sequence in italics (*WWAVAVSGEGFQTR*) showed 100% homology to PIP2 from *Brassica napus* and PIP2;1 from *Raphanus sativus*, both from the Brassicaceae family.

In 1997, two different genetic expression screening studies using Brassicaceae led to the identification of genes, called MIPB,[77] and MOD,[78] similar to PIP1 and with deduced amino acid sequences that include the peptide Q^{15}7YQALGGGANTVAPGYTK^{174}. *De novo* sequencing of the peptide with sequence QYQALGGGANTVAPGYTK (Table 3) allowed us to confirm the presence of PIP1;1. This result represents the first evidence of the expression of PIP1;1 isoform in roots, which agrees with the results of shown in Figure 1 after western-blot using the PIP1;1 antibody.

Identification of PIP Isoforms. In the case of aquaporins, a high degree of sequence homology usually hurdles the discrimination among PIP isoforms. As an example of this, 96.8% amino acid sequence homology is found between *At*PIP2;1 and *At*PIP2;2 isoforms. In the case of *B. oleracea*, the expression of two gene transcripts corresponding to PIP1 (*PIP1b1* and *PIP1b2*), differing only in a single amino acid (Ser^{78}-*PIP1b1* and Ala^{78}-*PIP1b2*), and highly homologous to PIP1;2 from *Arabidopsis*, have been described,[79] which leads to think that variations, even at the isoform level, can be found. Therefore, the identification of PIP isoforms is only possible upon identification of proteotypic peptides exclusively found in different PIP isoforms. For this reason, we aligned the amino acid sequences corresponding to the thirteen PIP isoforms

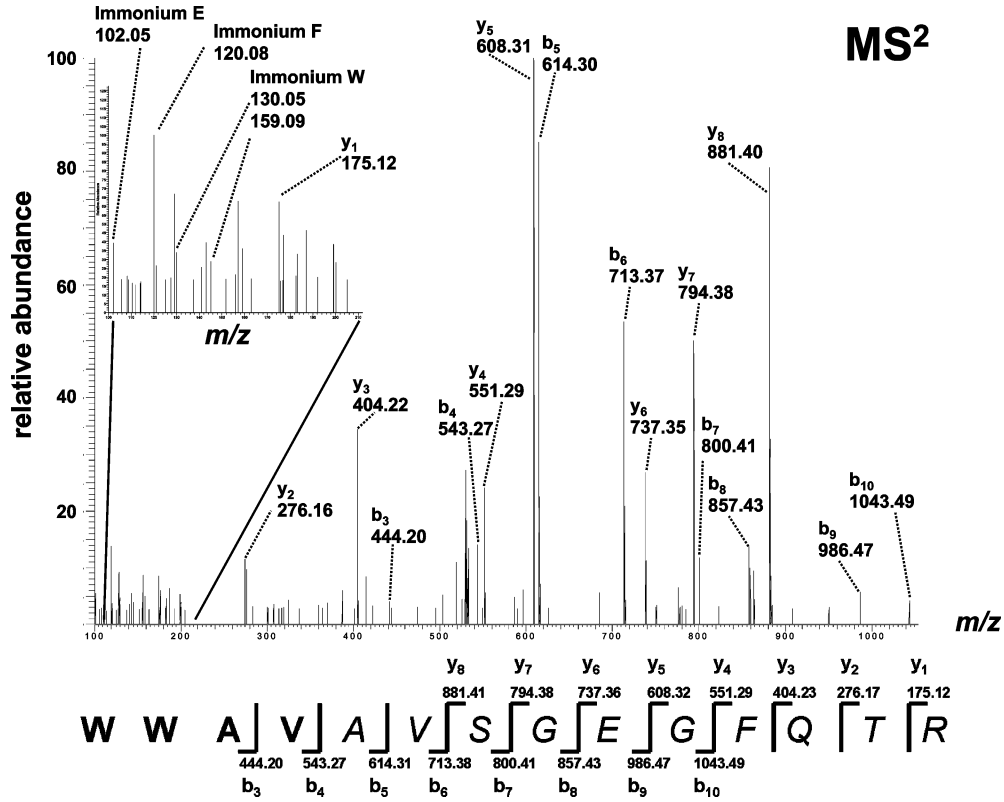

Figure 4. Example of a *de novo* sequenced peptide (m/z = 531.93) with sequence WWAV*AVSGEGFQTR*. A close-up view of the low mass region shows the presence of the y_1 fragment corresponding to R at the C-terminus and diagnostic ions for E (102.05), F (120.08) and W (130.05 and 159.09). The partial sequence in italics (*AVSGEGFQTR*) showed 100% homology to PIP2 from *Brassica napus* and PIP2;1 from *Raphanus sativus,* both from the Brassicaceae family.

described in *A. thaliana* (Figure 5). All the peptides sequences identified in our experiments, including database search and *de novo* sequencing, were also aligned in this figure. As depicted in this figure, the identification of the peptides with sequences Q[15]7YQALGGGANTVAHGYTK[174], S[239]LGAAIIFNK[248] and F[15]PERQPIGTSAQTDK[29] after CID fragmentation indicate the presence of PIP1;1, PIP1;2 and PIP1;3, respectively (Figure 5). The presence of the PIP2;2 and PIP 2;3 isoforms, were also confirmed after HCD fragmentation of the peptides D[15]YEDPPPTPFFDADELTK[32] and D[15]YEDPPPTPFFDAEELTK[32] respectively (Supplementary Table 1, Supporting Information). We also suggested the presence of two isoforms, PIP2;1 and PIP2;7 after the identification of the peptides D[4]VEAVSGEGFQTR[16] and T[142]PYNTLGGGANTVAPGYSK[160], each of them differing in only one amino acid (shown underlined) with the peptides D[4]VEAVPGEGFQTR[16] and T[142]PYNTLGGGANTVADGYSK[160], corresponding to PIP2;1 and PIP2;7 from *Arabidopsis*. One proteotypic peptide for PIP2;2 from *Petunia hybrida* was detected at m/z 1312.6532 assigned to the peptide with sequence SFGAAVIYNQDK. However, this mass might also be assigned to the peptide with sequence SFGAAVIYNNEK (Table 2). These two peptides, differing in two amino acid residues (shown underlined), shared similar MS/MS fragmentation spectra (Supplementary Figure 1A and B, Supporting Information) but eluted as two different peaks after HPLC separation of the peptides (Supplementary Figure 1C, Supporting Information). The last supports the identification of the two peptides.

Conclusions

To summarize, the strategy proposed here combining multiple endoprotease digestion followed by HPLC−MS/MS analysis facilitated the identification of PIPs isoforms and the characterization of their PTMs. If the species studied here was the model plant *A. thaliana*, the pool of peptides identified here would allow us to discern the occurrence of seven PIP isoforms.[1,4] Nevertheless, such a conclusion can not be drawn for broccoli, as the entire sequence of each broccoli PIP isoform is unknown. The impossibility to identify protein isoforms from *B. oleracea* is partly due to the lack of sequences from this species in the databases and justifies future sequencing projects focusing on plant species with agronomic and/or economic interest.

The finding of acetylation, phosphorylation and methylation on PIPs suggests that cytosolic N-acetyl transferases, kinases and methyl-transferases present in broccoli roots may possibly intervene in the regulation of plant PIPs activity.

Our results suggest that special care should be taken for the assignment of methylated residues on peptides from plant PIP proteins isolated from plant tissues when only HPLC−MS/MS analysis is used. The reason undermining the ability of HPLC−MS/MS to detect this modification is that several plant PIPs contain the motifs DE, EE, KD and KE. The dipeptides EE or DE_{me} share the same monoisotopic mass (276.09520 amu) and elemental composition ($C_{10}H_{16}N_2O_7$), which hampers their differentiation after mass spectrometric analysis, even if the masses of both, precursor and fragment ions, are measured with high mass accuracy in the Orbitrap analyzer. The same can be applied to the dipeptides KE and $K_{me}D$, also sharing the same monoisotopic mass (275.14757 amu) and elemental composition ($C_{11}H_{21}N_3O_5$). Although not frequently found in plant proteins, the possibility of finding Dme residues can not be ruled out. As recently described by Sprung et al.,[80] aspartic

Figure 5. Multiple sequence alignment of thirteen isoforms of PIP aquaporins from *A. thaliana*, including PIP1 and PIP2 subclasses, carried out with ClustalW. T. Swiss-Prot accession numbers and the full sequences of the five PIP1 isoforms (PIP1;1/PIP1;2/PIP1;3/PIP1;4/PIP1;5) and the eight PIP2 isoforms (PIP1;1/PIP1;2/PIP1;3/PIP1;4/PIP1;5) found in *A. thaliana* are shown. The position of the amino acids, starting from initial Met, is indicated with numbers. The position of the different PIP peptides identified in *B. oleracea* is also displayed. Regions in bold characters correspond to predicted trans-membrane regions using TMHMM and regions underlined correspond to re-entrant loops predicted with TMLoop. Ile/Leu ambiguity for *de novo* sequenced peptides is shown in italics (I/L).

methylation occurs in eukaryotic cells, but its identification through HPLC−MS/MS analysis has been has been largely overlooked.

The finding of a similar PIP modification pattern has also been described in the closely phylogenetically related species, *A. thaliana*. The highly conserved DNA sequences encoding for PIPs together with a repeated modification pattern found in PIPs from different tissues and from different species suggests that the regulation of PIP activity through PTMs may also be highly conserved within the Brassicaceae family.

Accurate detection in the Orbitrap analyzer of precursor ions and their corresponding MS/MS fragments after HCD fragmentation have been extendedly applied for peptide analysis[81,82] and in this work provided new peptide sequence information on broccoli root PIPs. The PIP peptides identified here, either after database search or by *de novo* sequencing provide the first pieces of information about the minimum number of isoforms present in broccoli roots. Peptides *de novo* sequenced also provide useful information to design primers to clone the specific genes encoding for PIP proteins in broccoli roots. The list of peptides identified and the description of isoform-specific proteotypic peptides may serve as a first stone for the design of peptide target analysis using more sensitive MS methods such as selected multiple reaction monitoring methods.[49] In order to make our data available for future studies, the output files containing the proteins identified and their corresponding peptides and post-translational modifications are available as Supporting Information (Supplementary excel files).

Finally, it has to underlined that the identification of PIP isoforms does not necessarily provide functional information on aquaporins (usually heteromers of different PIP isoforms); nevertheless, the fact that each isoform could play specific roles in various cell types, as they are differentially regulated in specific physiological contexts, turn the identification and characterization of PIPs in different plant species and the screening of their expression pattern in different organs useful tools to unravel the function and the regulation of PIPs in plants. We believe that the identification of PIP isoforms described here for *B. oleracea* could be the basis for further proteomics studies focusing on the regulation of PIPs and water balance that may eventually lead to the agronomical improvement of this crop.

Abbreviations: ACN, acetonitrile; AGC, automatic gain control; AQUA, absolute quantification strategy; BlastP, basic local alignment search tool for proteins; CID, collision induced dissociation; FDR, false discovery rate; fwhm, full width at half-maximum; HCD, higher-energy C-trap dissociation; MAPs, methionine aminopeptidases; MIP, major intrinsic protein; NIPs, NOD26-like intrinsic proteins; PAR, photosynthetically active radiation; PIPs, plasma membrane intrinsic proteins; PTMs, post-translational modifications; SIPs, small basic intrinsic proteins; TFA, trifluoroacetic acid; TIPs, tonoplast intrinsic proteins.

Acknowledgment. Mass spectrometry analysis was performed at CIC bioGUNE Proteomics Core Facility, member of CIBER-ehd and Proteored. This work was funded by the CICYT (AGL2006-06499) and the 'Consejería de Educación y Cultura de la Región de Murcia' ('BioCARM' BIO-AGR 06/04-0008). We thank Dr. Gorka Lasso for his kind contribution regarding bioinformatic tools and sequence alignment programs. We also thank Cassandra Wigmore, Lynette Lau and Janine Voyer (Bioinformatic Solutions) for their support in the use of Peaks software. M.C. Martínez-Ballesta thanks the Spanish Ministerio de Ciencia e Innovación and CSIC for funding through the "Ramón y Cajal" programme (ref RYC-2009-04574).

Supporting Information Available: Supplemental Figure 1. (A and B) MS/MS spectra corresponding to the peptides with sequence SFGAAVIYNQDK and SFGAAVIYNNEK detected at m/z 1312.65. Extracted ion chromatogram. (C) Extracted ion chromatogram showing the appearance of two peaks eluting after reversed phase separation of the peptides prior to MS analysis.Fragmentation spectra database searches against NCBI and Swiss-Prot after higher-energy C-trap dissociation (HCD) fragmentation. Supplemental Table 1. Zip file containg Excel files: Supplementary 1, TRYPSIN_NCBI; Supplementary 2, TRYPSIN_SWISSPROT; Supplementary 3, GLU-C_NCBI; Supplementary 4, GLU-C_SWISSPROT; Supplementary 5, LYS-C_NCBI 15; Supplementary 6, LYS-C_SWISSPROT; Supplementary 7, TIO2_NCBI; Supplementary 8, TIO2_SWISSPROT. This material is available free of charge via the Internet at http://pubs.acs.org.

References

(1) Maurel, C.; Javot, H.; Lauvergeat, V.; Gerbeau, P.; Tournaire, C.; Santoni, V.; Heyes, J. Molecular physiology of aquaporins in plants. *Int. Rev. Cytol.* **2002**, *215*, 105–148.
(2) Chaumont, F.; Barrieu, F.; Wojcik, E.; Chrispeels, M. J.; Jung, R. Aquaporins constitute a large and highly divergent protein family in maize. *Plant Physiol.* **2001**, *125*, 1206–1215.
(3) Johanson, U.; Gustavsson, S. A new subfamily of major intrinsic proteins in plants. *Mol. Biol. Evol.* **2002**, *19*, 456–461.
(4) Johanson, U.; Karlsson, M.; Johansson, I.; Gustavsson, S.; Sjovall, S.; Fraysse, L.; Weig, A. R.; Kjellbom, P. The complete set of genes encoding major intrinsic proteins in *Arabidopsis* provides a framework for a new nomenclature for major intrinsic proteins in plants. *Plant Physiol.* **2001**, *126*, 1358–1369.
(5) Smith, B. L.; Agre, P. Erythrocyte Mr 28,000 transmembrane protein exists as a multisubunit oligomer similar to channel proteins. *J. Biol. Chem.* **1991**, *266*, 6407–6415.
(6) Maurel, C. Plant aquaporins: novel functions and regulation properties. *FEBS Lett.* **2007**, *581*, 2227–2236.
(7) Martinez-Ballesta, M. C.; Silva, C.; Lopez-Berenguer, C.; Cabanero, F. J.; Carvajal, M. Plant aquaporins: new perspectives on water and nutrient uptake in saline environment. *Plant Biol.* **2006**, *8*, 535–546.
(8) Weig, A.; Deswarte, C.; Chrispeels, M. J. The major intrinsic protein family of *Arabidopsis* has 23 members that form three distinct groups with functional aquaporins in each group. *Plant Physiol.* **1997**, *114*, 1347–1357.
(9) Sakurai, J.; Ishikawa, F.; Yamaguchi, T.; Uemura, M.; Maeshima, M. Identification of 33 rice aquaporin genes and analysis of their expression and function. *Plant Cell Physiol.* **2005**, *46*, 1568–1577.
(10) Santoni, V.; Verdoucq, L.; Sommerer, N.; Vinh, J.; Pflieger, D.; Maurel, C. Methylation of aquaporins in plant plasma membrane. *Biochem. J.* **2006**, *400*, 189–197.
(11) Fischer, M.; Kaldenhoff, R. On the pH regulation of plant aquaporins. *J. Biol. Chem.* **2008**, *283*, 33889–33892.
(12) Nyblom, M.; Frick, A.; Wang, Y.; Ekvall, M.; Hallgren, K.; Hedfalk, K.; Neutze, R.; Tajkhorshid, E.; Tornroth-Horsefield, S. Structural and functional analysis of SoPIP2;1 mutants adds insight into plant aquaporin gating. *J. Mol. Biol.* **2009**, *387*, 653–668.
(13) Niittyla, T.; Fuglsang, A. T.; Palmgren, M. G.; Frommer, W. B.; Schulze, W. X. Temporal analysis of sucrose-induced phosphorylation changes in plasma membrane proteins of Arabidopsis. *Mol Cell. Proteomics* **2007**, *6*, 1711–1726.
(14) Prak, S.; Hem, S.; Boudet, J.; Viennois, G.; Sommerer, N.; Rossignol, M.; Maurel, C.; Santoni, V. Multiple phosphorylations in the C-terminal tail of plant plasma membrane aquaporins: role in subcellular trafficking of AtPIP2;1 in response to salt stress. *Mol. Cell Proteomics* **2008**, *7*, 1019–1030.
(15) Casado-Vela, J.; Rodriguez-Suarez, E.; Iloro, I.; Ametzazurra, A.; Alkorta, N.; García-Velasco, J. A.; Matorras, R.; Prieto, B.; González, S.; Nagore, D.; Simón, L.; Elortza, F. Comprehensive proteomic analysis of human endometrial fluid aspirate. *J. Proteome Res.* **2009**, *8*, 4622–4632.

(16) Alexandersson, E.; Saalbach, G.; Larsson, C.; Kjellbom, P. Arabidopsis plasma membrane proteomics identifies components of transport, signal transduction and membrane trafficking. *Plant Cell Physiol.* **2004**, *45*, 1543–1556.
(17) Santoni, V.; Vinh, J.; Pflieger, D.; Sommerer, N.; Maurel, C. A proteomic study reveals novel insights into the diversity of aquaporin forms expressed in the plasma membrane of plant roots. *Biochem. J.* **2003**, *373*, 289–296.
(18) Casado-Vela, J.; Ruiz, E. J.; Nebreda, A. R.; Casal, J. I. A combination of neutral loss and targeted product ion scanning with two enzymatic digestions facilitates the comprehensive mapping of phosphorylation sites. *Proteomics* **2007**, *7*, 2522–2529.
(19) Johansson, I.; Karlsson, M.; Shukla, V. K.; Chrispeels, M. J.; Larsson, C.; Kjellbom, P. Water transport activity of the plasma membrane aquaporin PM28A is regulated by phosphorylation. *Plant Cell* **1998**, *10*, 451–459.
(20) Han, J.; Schey, K. L. Proteolysis and mass spectrometric analysis of an integral membrane: aquaporin 0. *J. Proteome Res.* **2004**, *3*, 807–812.
(21) Hasegawa, P. M.; Bressan, R. A.; Zhu, J. K.; Bohnert, H. J. Plant cellular and molecular responses to high salinity. *Annu. Rev. Plant Physiol. Plant Mol. Biol.* **2000**, *51*, 463–499.
(22) Hoagland, D. R.; Arnon, D. I. The water culture method for growing plants without soil. *California Agr. Expt. Sta. Circ.* **1938**, *347*, 1–39.
(23) Larsson, C.; Widell, S.; Kjellbom, P. Preparation of high-purity plasma membranes. *Methods Enzymol.* **1987**, *148*, 558–568.
(24) Gerbeau, P.; Amodeo, G.; Henzler, T.; Santoni, V.; Ripoche, P.; Maurel, C. The water permeability of *Arabidopsis* plasma membrane is regulated by divalent cations and pH. *Plant J.* **2002**, *30*, 71–81.
(25) Widell, S.; Larsson, C. A critical evaluation of markers used in plasma membrane purification. In *The Plant Plasma Membranes: Structure, Function and Molecular Biology*; Larsson, C., Moller, I. M., Eds.; Springer-Verlag: Berlin, Germany, 1990; pp 16−43.
(26) O'Neill, S. D.; Bennett, A. B.; Spanswick, R. M. Characterization of a NO(3)-Sensitive H-ATPase from corn roots. *Plant Physiol.* **1983**, *72*, 837–846.
(27) Lundborg, T.; Widell, S.; Larsson, C. Distribution of ATPases in wheat root membranes separated by phase partition. *Physiol. Plant* **1981**, *52*, 89–95.
(28) Hodges, T. K.; Leonard, R. T. Purification of a plasma membrane-bound adenosine triphosphatase from plant roots. *Methods Enzymol.* **1974**, *32*, 392–406.
(29) Fotiadis, D.; Jeno, P.; Mini, T.; Wirtz, S.; Müller, S. A; Fraysse, L.; Kjellbom, P.; Engel, A. Structural characterization of two aquaporins isolated from native spinach leaf plasma membranes. *J. Biol. Chem.* **2001**, *276*, 1707–1714.
(30) Hasler, L.; Walz, T.; Tittmann, P.; Gross, H.; Kistler, J.; Engel, A. Purified lens major intrinsic protein (MIP) forms highly ordered tetragonal two-dimensional arrays by reconstitution. *J. Mol. Biol.* **1998**, *279*, 855–864.
(31) Towbin, H.; Staehelin, T.; Gordon, J. Electrophoretic transfer of proteins from polyacrylamide gels to nitrocellulose sheets: procedure and some applications. *Proc. Natl. Acad. Sci. U.S.A.* **1979**, *76*, 4350–4354.
(32) Kammerloher, W.; Fischer, U.; Piechottka, G. P.; Schaffner, A. R. Water channels in the plant plasma membrane cloned by immunoselection from a mammalian expression system. *Plant J.* **1994**, *6*, 187–199.
(33) Casado-Vela, J.; Martinez-Torrecuadrada, J. L.; Casal, J. I. Differential phosphorylation patterns between the Cyclin-A2/CDK2 complex and their monomers. *Protein Expr. Purif.* **2009**, *66*, 15–21.
(34) Shevchenko, A.; Wilm, M.; Vorm, O.; Mann, M. Mass spectrometric sequencing of proteins silver-stained polyacrylamide gels. *Anal. Chem.* **1996**, *68*, 850–858.
(35) Thingholm, T. E.; Jorgensen, T. J.; Jensen, O. N.; Larsen, M. R. Highly selective enrichment of phosphorylated peptides using titanium dioxide. *Nat. Protoc.* **2006**, *1*, 1929–1935.
(36) Eng, J. K.; McCormack, M.; Yates, J. R. An approach to correlate tandem spectral data of peptides with amino sequences in a protein database. *J. Am. Soc. Mass Spectrom.* **1994**, *5*, 976–989.
(37) Thompson, J. D.; Higgins, D. G.; Gibson, T. J. CLUSTAL W: improving the sensitivity of progressive multiple sequence alignment through sequence weighting, position-specific gap penalties and weight matrix choice. *Nucleic Acids Res.* **1994**, *22*, 4673–4680.
(38) Krogh, A.; Larsson, B.; von Heijne, G.; Sonnhammer, E. L. Predicting transmembrane protein topology with a hidden Markov model: application to complete genomes. *J. Mol. Biol.* **2001**, *305*, 567–580.
(39) Lasso, G.; Antoniw, J. F.; Mullins, J. G. A combinatorial pattern discovery approach for the prediction of membrane dipping (re-entrant) loops. *Bioinformatics* **2006**, *22*, e290–e297.
(40) Kjellbom, P.; Larsson, C.; Johansson, I. I.; Karlsson, M.; Johanson, U. Aquaporins and water homeostasis in plants. *Trends Plant Sci.* **1999**, *4*, 308–314.
(41) Buck, T. M.; Eledge, J.; Skach, W. R. Evidence for stabilization of aquaporin-2 folding mutants by N-linked glycosylation in endoplasmic reticulum. *Am. J. Physiol. Cell Physiol.* **2004**, *287*, C1292–1299.
(42) Zeidel, M. L.; Ambudkar, S. V.; Smith, B. L.; Agre, P. Reconstitution of functional water channels in liposomes containing purified red cell CHIP28 protein. *Biochemistry* **1992**, *31*, 7436–7440.
(43) Hirano, K.; Zuber, C.; Roth, J.; Ziak, M. The proteasome is involved in the degradation of different aquaporin-2 mutants causing nephrogenic diabetes insipidus. *Am. J. Pathol.* **2003**, *163*, 111–120.
(44) Leitch, V.; Agre, P.; King, L. S. Altered ubiquitination and stability of aquaporin-1 in hypertonic stress. *Proc. Natl. Acad. Sci. U.S.A.* **2001**, *98*, 2894–2898.
(45) Han, Z. B.; Yang, J. B.; Wax, M. B.; Patil, R. V. Molecular identification of functional water channel protein in cultured human nonpigmented ciliary epithelial cells. *Curr. Eye Res.* **2000**, *20*, 242–247.
(46) Borgnia, M. J.; Kozono, D.; Calamita, G.; Maloney, P. C.; Agre, P. Functional reconstitution and characterization of AqpZ, the *E. coli* water channel protein. *J. Mol. Biol.* **1999**, *291*, 1169–1179.
(47) Marmagne, A.; Rouet, M. A.; Ferro, M.; Rolland, N.; Alcon, C.; Joyard, J.; Garin, J.; Barbier-Brygoo, H.; Ephritikhine, G. Identification of new intrinsic proteins in *Arabidopsis* plasma membrane proteome. *Mol. Cell. Proteomics* **2004**, *3*, 675–691.
(48) Natera, S. H.; Ford, K. L.; Cassin, A. M.; Patterson, J. H.; Newbigin, E. J.; Bacic, A. Analysis of the *Oryza sativa* plasma membrane proteome using combined protein and peptide fractionation approaches in conjunction with mass spectrometry. *J. Proteome Res.* **2008**, *7*, 1159–1187.
(49) Altschul, S. F.; Madden, T. L.; Schaffer, A. A.; Zhang, J.; Zhang, Z.; Miller, W.; Lipman, D. J. Gapped BLAST and PSI-BLAST: a new generation of protein database search programs. *Nucleic Acids Res.* **1997**, *25*, 3389–3402.
(50) Kyte, J.; Doolittle, R. F. A simple method for displaying the hydropathic character of a protein. *J. Mol. Biol.* **1982**, *157*, 105–132.
(51) Cao, R.; He, Q.; Zhou, J.; He, Q.; Liu, Z.; Wang, X.; Chen, P.; Xie, J.; Liang, S. High-throughput analysis of rat liver plasma membrane proteome by a nonelectrophoretic in-gel tryptic digestion coupled with mass spectrometry identification. *J. Proteome Res.* **2008**, *7*, 535–545.
(52) Meinnel, T.; Peynot, P.; Giglione, C. Processed N-termini of mature proteins in higher eukaryotes and their major contribution to dynamic proteomics. *Biochimie* **2005**, *87*, 701–712.
(53) Polevoda, B.; Sherman, F. Nalpha -terminal acetylation of eukaryotic proteins. *J. Biol. Chem.* **2000**, *275*, 36479–36482.
(54) Polevoda, B.; Sherman, F. N-terminal acetyltransferases and sequence requirements for N-terminal acetylation of eukaryotic proteins. *J. Mol. Biol.* **2003**, *325*, 595–622.
(55) Flinta, C.; Persson, B.; Jornvall, H.; von Heijne, G. Sequence determinants of cytosolic N-terminal protein processing. *Eur. J. Biochem.* **1986**, *154*, 193–196.
(56) Larsen, M. R.; Thingholm, T. E.; Jensen, O. N.; Roepstorff, P.; Jorgensen, T. J. Highly selective enrichment of phosphorylated peptides from peptide mixtures using titanium dioxide microcolumns. *Mol. Cell. Proteomics* **2005**, *4*, 873–886.
(57) Molina, H.; Horn, D. M.; Tang, N.; Mathivanan, S.; Pandey, A. Global proteomic profiling of phosphopeptides using electron transfer dissociation tandem mass spectrometry. *Proc. Natl. Acad. Sci. U.S.A.* **2007**, *104*, 2199–2204.
(58) Mazanek, M.; Mituloviae, G.; Herzog, F.; Stingl, C.; Hutchins, J. R.; Peters, J. M.; Mechtler, K. Titanium dioxide as a chemo-affinity solid phase in offline phosphopeptide chromatography prior to HPLC-MS/MS analysis. *Nat. Protoc.* **2007**, *2*, 1059–1069.
(59) Pinkse, M. W.; Uitto, P. M.; Hilhorst, M. J.; Ooms, B.; Heck, A. J. Selective isolation at the femtomole level of phosphopeptides from proteolytic digests using 2D-NanoLC-ESI-MS/MS and titanium oxide precolumns. *Anal. Chem.* **2004**, *76*, 3935–3943.
(60) Gonen, T.; Cheng, Y.; Kistler, J.; Walz, T. Aquaporin-0 membrane junctions form upon proteolytic cleavage. *J. Mol. Biol.* **2004**, *342*, 1337–1345.
(61) Murata, K.; Mitsuoka, K.; Hirai, T.; Walz, T.; Agre, P.; Heymann, J. B.; Engel, A.; Fujiyoshi, Y. Structural determinants of water permeation through aquaporin-1. *Nature* **2000**, *407*, 599–605.

(62) Sui, H.; Han, B. G.; Lee, J. K.; Walian, P.; Jap, B. K. Structural basis of water-specific transport through the AQP1 water channel. *Nature* **2001**, *414*, 872–878.
(63) Fischer, G.; Kosinska-Eriksson, U.; Aponte-Santamaria, C.; Palmgren, M.; Geijer, C.; Hedfalk, K.; Hohmann, S.; de Groot, B. L.; Neutze, R.; Lindkvist-Petersson, K. Crystal structure of a yeast aquaporin at 1.15 angstrom reveals a novel gating mechanism. *PLoS Biol.* **2009**, *7*, e1000130.
(64) Tornroth-Horsefield, S.; Wang, Y.; Hedfalk, K.; Johanson, U.; Kjellbom, P.; Neutze, R. Structural mechanism of plant aquaporin gating. *Nature* **2006**, *439*, 688–694.
(65) Azad, A. K.; Katsuhara, M.; Sawa, Y.; Ishikawa, T.; Shibata, H. Characterization of four plasma membrane aquaporins in tulip petals: A putative homolog is regulated by phosphorylation. *Plant Cell Physiol.* **2008**, *49*, 1196–1208.
(66) Tournaire-Roux, C.; Sutka, M.; Javot, H.; Gout, E.; Gerbeau, P.; Luu, D. T.; Bligny, R.; Maurel, C. Cytosolic pH regulates root water transport during anoxic stress through gating of aquaporins. *Nature* **2003**, *425*, 393–397.
(67) Gunnarson, E.; Zelenina, M.; Axehult, G.; Song, Y.; Bondar, A.; Krieger, P.; Brismar, H.; Zelenin, S.; Aperia, A. Identification of a molecular target for glutamate regulation of astrocyte water permeability. *Glia* **2008**, *56*, 587–596.
(68) Guenther, J. F.; Chanmanivone, N.; Galetovic, M. P.; Wallace, I. S.; Cobb, J. A.; Roberts, D. M. Phosphorylation of soybean nodulin 26 on serine 262 enhances water permeability and is regulated developmentally and by osmotic signals. *Plant Cell* **2003**, *15*, 981–991.
(69) Maurel, C.; Kado, R. T.; Guern, J.; Chrispeels, M. J. Phosphorylation regulates the water channel activity of the seed-specific aquaporin alpha-TIP. *EMBO J.* **1995**, *14*, 3028–3035.
(70) Maurel, C.; Tacnet, F.; Guclu, J.; Guern, J.; Ripoche, P. Purified vesicles of tobacco cell vacuolar and plasma membranes exhibit dramatically different water permeability and water channel activity. *Proc. Natl. Acad. Sci. U.S.A.* **1997**, *94*, 7103–7108.
(71) Suga, S.; Maeshima, M. Water channel activity of radish plasma membrane aquaporins heterologously expressed in yeast and their modification by site-directed mutagenesis. *Plant Cell Physiol.* **2004**, *45*, 823–830.
(72) Gerber, S. A.; Rush, J.; Stemman, O.; Kirschner, M. W.; Gygi, S. P. Absolute quantification of proteins and phosphoproteins from cell lysates by tandem MS. *Proc. Natl. Acad. Sci. U.S.A.* **2003**, *100*, 6940–6945.
(73) Johansson, I.; Larsson, C.; Ek, B.; Kjellbom, P. The major integral proteins of spinach leaf plasma membranes are putative aquaporins and are phosphorylated in response to Ca^{2+} and apoplastic water potential. *Plant Cell.* **1996**, *8*, 1181–1191.
(74) Nuhse, T. S.; Stensballe, A.; Jensen, O. N.; Peck, S. C. Phosphoproteomics of the *Arabidopsis* plasma membrane and a new phosphorylation site database. *Plant Cell.* **2004**, *16*, 2394–2405.
(75) Cox, J.; Hubner, N. C.; Mann, M. How much peptide sequence information is contained in ion trap tandem mass spectra. *J. Am. Soc. Mass Spectrom.* **2008**, *19*, 1813–1820.
(76) Pevtsov, S.; Fedulova, I.; Mirzaei, H.; Buck, C.; Zhang, X. Performance evaluation of existing de novo sequencing algorithms. *J. Proteome Res.* **2006**, *5*, 3018–3028.
(77) Ruiter, R. K.; Van Eldik, G. J.; van Herpen, M. M.; Schrauwen, J. A.; Wullems, G. J. Expression in anthers of two genes encoding *Brassica oleracea* transmembrane channel proteins. *Plant Mol. Biol.* **1997**, *34*, 163–168.
(78) Ikeda, S.; Nasrallah, J. B.; Dixit, R.; Preiss, S.; Nasrallah, M. E. An aquaporin-like gene required for the *Brassica* self-incompatibility response. *Science* **1997**, *276*, 1564–1566.
(79) Marin-Olivier, M.; Chevalier, T.; Fobis-Loisy, I.; Dumas, C.; Gaude, T. Aquaporin PIP genes are not expressed in the stigma papillae in *Brassica oleracea*. *Plant J.* **2000**, *24*, 231–240.
(80) Sprung, R.; Chen, Y.; Zhang, K.; Cheng, D.; Zhang, T.; Peng, J.; Zhao, Y. Identification and validation of eukaryotic aspartate and glutamate methylation in proteins. *J. Proteome Res.* **2008**, *7* (3), 1001–1006.
(81) Olsen, J. V.; Macek, B.; Lange, O.; Makarov, A.; Horning, S.; Mann, M. Higher-energy C-trap dissociation for peptide modification analysis. *Nat. Methods* **2007**, *4*, 709–712.
(82) Yates, J. R.; Ruse, C. I.; Nakorchevsky, A. Proteomics by mass spectrometry: approaches, advances and applications. *Annu. Rev. Biomed. Eng.* **2009**, *11*, 49–79.

PR901150G